Development of a General Mathematical Framework for Modeling Diffusion-Controlled Free-Radical Polymerization Reactions

D. S. Achilias and C. Kiparissides*

Department of Chemical Engineering, Chemical Process Engineering Research Institute, Aristotle University of Thessaloniki, P.O. Box 472, 540 06 Thessaloniki, Greece

Received September 16, 1991; Revised Manuscript Received March 5, 1992

ABSTRACT: A new theoretical framework is proposed for modeling diffusion-controlled free-radical polymerization reactions. Termination and propagation rate constants as well as initiator efficiency are expressed in terms of a reaction-limited term and a diffusion-limited one. The latter is shown to depend on the diffusion coefficient of the corresponding species (i.e., polymer, monomer, primary radicals) and an effective reaction radius. All parameters appearing in the diffusion-limited part of the kinetic rate constants have a clear physical meaning and can be evaluated in terms of the physical and transport properties of the reacting species. It is shown that the proposed approach for modeling diffusion-controlled reactions does not require the introduction of critical break points to mark the onset of various diffusional effects (i.e., gel effect, glass effect). The ability of the present model to elucidate the mechanism of diffusion-controlled reactions is demonstrated by analyzing the free-radical polymerizations of styrene and methyl methacrylate initiated by the thermal decomposition of AIBN, AIBME, AVN, and LPO chemical initiators. It is shown that, at high conversions, initiator efficiency strongly depends on the size of initiator molecules. The present model predictions are in excellent agreement with experimental data on monomer conversion, total radical concentration, and average molecular weights measured in different laboratories by O'Driscoll and Huang[42] and Zhu et al.[10]

Introduction

Besides the conventional chemical kinetics, physical phenomena related to the diffusion of various chemical reactive species are very important in free-radical polymerizations. In fact, at high monomer conversions, almost all elementary reactions can become diffusion-controlled. Reactions which are influenced by diffusion phenomena include termination of "live" macroradicals, propagation of a growing chain, and chemical initiation reactions.

Diffusion-controlled termination, propagation, and initiation reactions have been related to the well-known phenomena of gel effect, glass effect, and cage effect, respectively. In the past 20 years, several models have been published dealing with the mathematical description of diffusion-controlled kinetic rate constants in free-radical polymerizations.

The gel effect, or Trommsdorff–Norrish effect, has been attributed to the decrease of the termination rate constant caused by a decrease of the mobility of polymer chains. This phenomenon strongly affects the final polymer properties, since it leads to a broader molecular weight distribution. It can also cause the thermal runaway of a polymerization reactor. There are a great number of publications dealing with the mathematical description of the gel effect. These have been recently reviewed by Achilias and Kiparissides[1] and Mita and Horie.[2]

The glass effect has been related to the decrease of the propagation rate constant caused by a decrease of the mobility of the monomer molecules. The glass effect appears in polymerizations taking place at temperatures below the glass transition temperature of the polymer. A consequence of this phenomenon is the "freezing" of the reaction mixture at conversions below 100%. At the limiting conversion, the glass transition temperature of the polymer/monomer mixture becomes equal to the polymerization temperature. Diffusion-controlled propagation reactions have been modeled by several investigators and have been reviewed by Achilias and Kiparissides[1] and Mita and Horie.[2]

Chemical initiation involves the decomposition of initiator molecules to form very active primary radicals capable of initiating new polymer chains. However, due to the very close proximity of the generated radicals, not all of them can eventually escape from their "cages" to react with monomer molecules. In fact, some primary radicals will either self-terminate or react with other nearest-neighboring molecules before diffusing out of their "cages". The concept of a primary radical "cage" formed by neighboring molecules (i.e., growing radicals, polymer chains, solvent molecules) surrounding the new generated radicals was first introduced by Frank and Rabinowitch[3,4] and later modeled by Noyes.[5,6] To account for this phenomenon, they introduced an empirical parameter, f, called the initiator efficiency factor, which represents the fraction of all generated initiator primary radicals leading to formation of new polymer chains. This parameter can take values in the range 0–1. Whether or not the efficiency factor remains constant during a polymerization is still a subject of discussion and present research activities. In a great number of papers, f has been treated as a constant parameter. Indeed, experimental results reported by Brooks[7] provided some evidence for a constant initiator efficiency. However, De Schrijver and Smets[8] found that the initiator efficiency was slightly decreased at high conversions due to the increase of the viscosity of the reaction medium.

Recent experimental results[9–11] show that initiator efficiency can dramatically change with monomer conversion. This indicates that diffusion of primary radicals will be influenced by the physical and transport properties of the reaction medium.

The first theoretical models on the prediction of initiator efficiency were based on the assumption that kinetic limitations rather than diffusion phenomena were responsible for the observed decrease in f during polymerization.[12–14] Arai and Saito[15,16] first pointed out the importance of diffusional phenomena in modeling the change of initiator efficiency in free-radical bulk polymerizations. They employed the generalized free-volume theory to calculate the variation of the diffusion coefficient of primary radicals in the reaction medium. However, it should be pointed out that some parameters in Arai and

0024-9297/92/2225-3739$03.00/0

Saito's model were determined by fitting model predictions to experimental data.

Stickler[17] studied the polymerization kinetics of the BzO_2/MMA system near its glassy point and found that the initiator efficiency varied in the range 0.1–0.2. An attempt to model the cage effect was also presented by Denisov.[18] He concluded that both rotational and translational motion of initiator primary radicals could influence this phenomenon. In 1985, Ito[19] developed a model to describe the cage effect in free-radical polymerizations and proposed an equation for the estimation of initiator efficiency. An elaborate theory describing the decrease of initiator efficiency at high conversions was presented by Russell et al.[20] They were able to calculate f from experimental data and proved that f was independent of initiator concentration although it depended on initiator type. They also pointed out that f could decrease by many orders of magnitude beyond a critical conversion marking the abrupt change of physical and chemical properties of the system. Zhu and Hamielec[21] utilized Balke's[22] experimental data to show the existence of a dramatic change in initiator efficiency near the glassy state of the reacting mixture.

Recent advances in analytical techniques for the measurement of the total live radical concentration have given a new insight to the experimental determination of the initiator efficiency. Ballard et al.[23] used an electron spin resonance (ESR) spectrometer to measure the variation of the propagation rate constant in the emulsion polymerization of MMA. The use of the ESR technique for the direct measurement of radical concentration has been reviewed by Kamachi.[24] Shen et al.[25] first measured directly the total radical concentration in the bulk polymerization of MMA. They were actually able to verify experimentally the increase in the radical population during the autoacceleration of the polymerization rate. Later, Zhu et al.[10] using ESR measured the radical concentration in the free-radical bulk copolymerization of MMA/EGDMA over the entire conversion range. The same authors, in a later publication,[26] were able to measure experimentally the average termination rate constant throughout the course of the reaction.

Almost all models appearing in the literature contain a number of adjustable parameters estimated by fitting model predictions to experimental data. Moreover, critical break points are often introduced to mark the onset of different diffusional processes occurring during polymerization. In the present work, an attempt is made to develop a general framework for modeling the diffusion-controlled termination and propagation rate constants as well as to predict the variation of initiator efficiency with monomer conversion. The diffusion models presented in this work are based on a mathematical representation of the physical phenomena taking place during the polymerization and contain no adjustable parameters. All models describing the diffusion-controlled kinetics of the various elementary reactions of interest consist of a reaction-limited term and a diffusional one. No critical break points are required to mark the onset of the various diffusional effects. The ability of the new theoretical framework to describe diffusion-controlled phenomena in free-radical polymerizations is demonstrated by analyzing several polymerization systems, including the bulk polymerization of methyl methacrylate and styrene. To our knowledge this is the first attempt to predict the variation of radical concentration as well as conversion and average molecular weights during polymerization by taking into account simultaneously the diffusion-controlled dependence of all three kinetic parameters k_t, k_p, and f on the polymerization conditions.

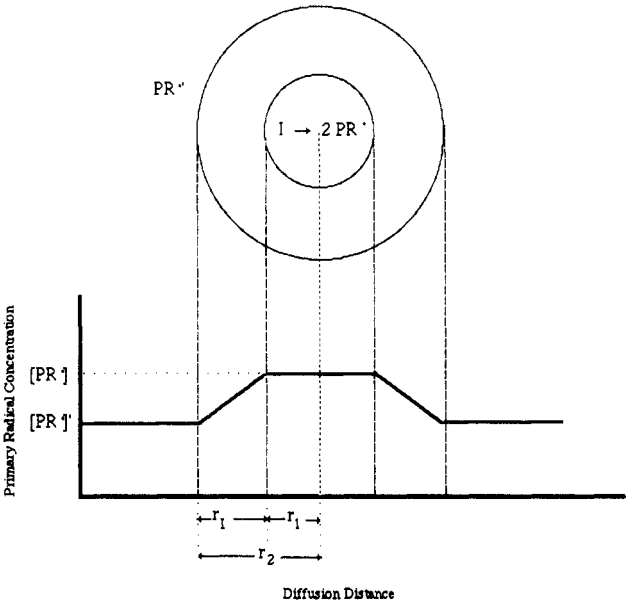

Figure 1. Schematic diagram illustrating the coordinate system used in describing the primary radical diffusion process.

Diffusion-Controlled Initiation Reaction

The thermal decomposition of initiator is assumed to proceed according to the following kinetic mechanism:

Primary Radical Initiation

$$I \xrightarrow{k_d} 2PR^{\bullet} + G\uparrow \quad (1)$$

Primary Radical Deactivation

$$PR^{\bullet} + PR^{\bullet} \xrightarrow{k_c} I' \quad (2)$$

Polymer Chain Initiation

$$PR^{\bullet} + M \xrightarrow{k_i} P^{\bullet}_1 \quad (3)$$

All reactions are considered to be elementary and irreversible. According to the "cage" modeling concept elaborated above, the various molecular species in the reaction medium form around the primary radicals, PR·, a cell which inhibits their diffusion. As a result, only a fraction of the generated radicals succeed in escaping from the cage to initiate new polymer chains.

The primary radical diffusion rate will depend on the diffusion coefficient of the radicals, D_I, as well as the viscosity and temperature of the reaction medium. Following a modeling approach similar to the one described in our previous article,[1] the primary radical cage is approximated by two concentric spheres of radii r_1 and r_2 (Figure 1). It is assumed that primary radicals are only generated in the initiator reaction sphere of radius r_1, placed inside the larger diffusion sphere of radius r_2, shown schematically in Figure 1. Only radicals escaping from the diffusion sphere of radius r_2 can react with monomer to initiate new polymer chains.

Let $[PR^{\bullet}]'$ be an effective concentration of primary radicals outside the diffusion sphere, r_2. The distance that primary radicals have to travel to escape from the

cage will be $r_I = r_2 - r_1$. Assuming a one-dimensional steady-state mass transfer process, the diffusion rate of primary radicals out of the cage will be equal to the extensive chain initiation reaction rate between monomer and escaping primary radicals, R'_I:

$$-4\pi r^2 D_I \frac{d[R^\bullet]}{dr} = R'_I \quad (4)$$

Equation 4 will satisfy the following boundary conditions:

$$[R^\bullet] = [PR^\bullet], \quad r = r_1$$

$$[R^\bullet] = [PR^\bullet]', \quad r = r_2 \quad (5)$$

integrating eq 4 from r_1 to r_2 and assuming that $r_2 \gg r_1$, we obtain

$$D_I(4\pi r_1)([PR^\bullet] - [PR^\bullet]') = R'_I \quad (6)$$

According to eq 3, the extensive chain initiation reaction rate, R'_I, will be given by

$$R'_I = k_{i0}[PR^\bullet]'[M]V_I \quad (7)$$

where k_{i0} is the intrinsic chain initiation rate constant and $[PR^\bullet]'$ is the effective primary radical concentration. V_I denotes an effective chain initiation reaction volume and is assumed to be equal to $4\pi r_2^3/3$. From eqs 6 and 7, one can estimate the effective primary radical concentration $[PR^\bullet]'$ in terms of $[PR^\bullet]$, $[M]$, D_I, k_{i0}, and the radii r_1 and r_2.

$$[PR^\bullet]/[PR^\bullet]' = [1 + k_{i0}[M]r_2^3/(3r_1D_I)] \quad (8)$$

Assuming that the quasi-steady-state approximation (QSSA) for primary radicals holds true, one can express the extensive chain initiation reaction rate as

$$R_I = k_{i0}[PR^\bullet]'[M] = 2fk_d[I] \quad (9)$$

or at very low conversions

$$R_I = k_{i0}[PR^\bullet][M] = 2f_0k_d[I] \quad (10)$$

where f_0 and f denote the initial initiator efficiency (at $t = 0$) and the time-varying initiator efficiency, respectively. Dividing eqs 9 and 10 and substituting eq 8 into the resulting expression, we obtain

$$\frac{1}{f} = \frac{1}{f_0} + \frac{r_2^3}{3r_1}\frac{k_{i0}}{f_0}\frac{[M]}{D_I} \quad (11)$$

As shown later, the functional form of eq 11 is similar to that of eqs 30 and 48 describing the variation of the termination and the propagation rate constants with conversion. In fact, eq 11 accounts for both chemical (i.e., intrinsic initiator efficiency) and physical (i.e., primary radical diffusion) phenomena affecting the overall initiator efficiency during polymerization.

To obtain a relative measure of the importance of the two terms in eq 11, we introduce two characteristic time constants, τ_{DI} and τ_{RI}:

$$\tau_{DI} = (r_2^3/3r_1D_I) \qquad \tau_{RI} = (k_{i0}[M])^{-1} \quad (12)$$

τ_{DI} and τ_{RI} are the characteristic times related to the diffusion of primary radicals and the chain initiation reaction 3, respectively. From eq 11 and the definitions of τ_{DI} and τ_{RI}, the initiator efficiency can be expressed as

$$f = f_0/(1 + \tau_{DI}/\tau_{RI}) \quad (13)$$

Note that the initiator efficiency, f, will depend on the ratio τ_{DI}/τ_{RI}. Thus, if diffusion of primary radicals is important (i.e., $\tau_{DI} \gg \tau_{RI}$), then the initiator efficiency, f, will be smaller than f_0:

$$\tau_{DI} \gg \tau_{RI}, \quad f < f_0 \quad (14)$$

On the other hand, if the characteristic time for chain initiation, τ_{RI}, is greater than τ_{DI}, then the initiator efficiency will remain constant:

$$\tau_{DI} \ll \tau_{RI}, \quad f \approx f_0 \quad (15)$$

According to eq 11, for the calculation of f one needs to know the values of the parameters, D_I, $r_2^3/3r_1$, and k_{i0}. In what follows, theoretical expressions are derived which make possible the analytical estimation of these parameters from the physical and transport properties of the reacting system.

Calculation of the Primary Radical Diffusion Coefficient D_I. The calculation of D_I is based on the generalized free-volume theory of Vrentas and Duda.[27,28] According to the cage model described above, primary radicals diffuse into an environment consisting of monomer molecules as well as macromolecules (i.e., "live" macroradicals and "dead" polymer molecules), which means that diffusion occurs into a ternary solution. The diffusion coefficient of primary radicals can be expressed according to Vrentas et al.[29] as

$$D_I = D_{I0}\exp[-\gamma(\omega_m\hat{V}_m^*\xi_{23}/\xi_{13} + \omega_I\hat{V}_I^* + \omega_p\hat{V}_p^*\xi_{23})/\hat{V}_f] \quad (16)$$

where

$$\hat{V}_f = \omega_m\hat{V}_m^*V_{fm} + \omega_I\hat{V}_I^*V_{fI} + \omega_p\hat{V}_p^*V_{fp} \quad (17)$$

$$\xi_{i3} = (\hat{V}_i^*M_{ji})/(\hat{V}_p^*M_{jp}), \quad i = 1, 2, 3 \quad (18)$$

The subscript i identifies the monomer (1), initiator (2), and polymer chains (3). Assuming that the weight fraction of primary radicals (ω_I) is very small compared to the corresponding weight fractions of monomer and polymer, eq 16 reduces to

$$D_I = D_{I0}\exp[-\gamma(\omega_m\hat{V}_m^*\xi_{23}/\xi_{13} + \omega_p\hat{V}_p^*\xi_{23})/\hat{V}_f] \quad (19)$$

$$\hat{V}_f = \omega_m\hat{V}_m^*V_{fm} + \omega_p\hat{V}_p^*V_{fp} \quad (20)$$

Substituting eq 18 into eq 19, we obtain

$$D_I = D_{I0}\exp[-\gamma\hat{V}_I^*M_{jI}[(\omega_m/M_{jm}) + (\omega_p/M_{jp})]/\hat{V}_f] \quad (21)$$

All symbols are explained in the Nomenclature. For the calculation of D_I from eq 21, one needs to know the values of the physical parameters of the monomer–polymer system (M_{jm}, M_{jp}, V_{fm}, V_{fp}, $\hat{V}_m^*$, $\hat{V}_p^*$) and the values of the parameters ($\hat{V}_I^*$, M_{jI}, γ, D_{I0}) related to the initiator molecules. The first set of parameters is calculated according to the generalized free-volume theory of Vrentas and Duda.[27,28] The latter set includes the specific initiator volume, $\hat{V}_I^*$, which is estimated according to Haward,[30] the molecular weight of the initiator fragment, M_{jI}, the initiator overlap factor, γ, and the diffusion coefficient of the primary radicals, D_{I0}. Unfortunately, there are no available data in the open literature with respect to the last two parameters (γ, D_{I0}). In the present work, the value of γ was taken equal to 1 for all types of initiators. The estimation of D_{I0} is discussed next.

To examine the validity of the assumption $D_I = D_m$ that was originally proposed by Russell et al.,[20] we first derive an expression for the monomer diffusion coefficient in a ternary solution. Following the theoretical developments of Vrentas et al.[29] D_m is expressed as

$$D_m = D_{m0}\exp[-\gamma(\omega_m\hat{V}_m^* + \omega_I\hat{V}_I^*\xi_{13}/\xi_{23} + \omega_p\hat{V}_p^*\xi_{13})/\hat{V}_f] \quad (22)$$

For small values of ω_I, eq 22 is reduced to

$$D_m = D_{m0} \exp[-\gamma(\omega_m \hat{V}_m^* + \omega_p \hat{V}_p^* \xi_{13})/\hat{V}_f] \quad (23)$$

Substituting eq 18 into eq 23 yields

$$D_m = D_{m0} \exp[-\gamma \hat{V}_m^* M_{jm}[(\omega_m/M_{jm}) + (\omega_p/M_{jp})]/\hat{V}_f] \quad (24)$$

Finally, from eqs 21 and 24 we obtain

$$\ln \frac{D_I}{D_{I0}} = [(\hat{V}_I^* M_{jI})/(\hat{V}_m^* M_{jm})] \ln \frac{D_m}{D_{m0}} \quad (25)$$

Note that the diffusion coefficient of the primary radical, D_I, will be equal to the diffusion coefficient of the monomer, D_m, if the following equation is satisfied:

$$\hat{V}_I^* M_{jI} = \hat{V}_m^* M_{jm} \quad (26)$$

It should be pointed that D_I and, implicitly, the initiator efficiency will depend on the molecular weight of the diffusing radical, M_{jI}. Thus, as the molecular weight of the primary radical increases, the diffusion coefficient decreases (see eq 21) as well as the initiator efficiency according to equ 11. Russell et al.[20] obtained the same qualitative results but they did not offer a quantitative explanation.

Calculation of k_{i0}. k_{i0} is the intrinsic kinetic rate constant for the chain initiation reaction 3. Its value will depend on the type of initiator and monomer molecules and will obey an Arrhenius equation with respect to the polymerization temperature. To our knowledge there are no available data on k_{i0} for various monomer–initiator systems. However, for the AIBME-initiated MMA polymerization, the molecular structure of the primary radical (PR•) resembles that of the chain end of the polymeric radical:[31]

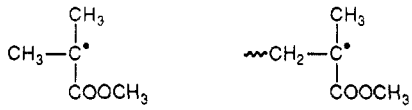

Therefore, it is reasonable to assume that the propagation rate constant k_{p0} will be equal to the chain initiation rate constant k_{i0}. For the same system AIBME/MMA, one can assume that $D_I \cong D_m$.

For the AIBN-initiated MMA polymerization, the molecular structure of the primary radicals is

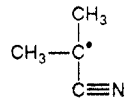

Since the structure of the two radicals (i.e., primary and growing polymer chains) is not very different, we can assume that the following relationship between k_{i0} and k_{p0} will hold true:

$$k_{i0} = \epsilon_i k_{p0} \quad (27)$$

where ϵ_i is a proportionality constant. In the present work, the ratio ϵ_i/D_{I0} is treated as a single unknown parameter. Its value is estimated from the application of the following initial condition:

$$f = f_0, \quad x = 0 \quad (28)$$

Calculation of $r_2^3/(3r_1)$. The term $r_2^3/(3r_1)$ contains the geometrical features of the cage. Assuming that the initiator fragments are not very different in size from the monomer molecules, r_1 can be approximated by the diameter of a monomer molecule.

$$r_1 = (6V_m/\pi N_A)^{1/3} \quad (29)$$

Assuming that $D_I \cong D_m$ and $k_{i0} \cong k_{p0}$, the value of r_2 was found to be equal to the initial hydrodynamic diameter of the polymer. Thus, the expression $r_2 = 2(R_H)_0$ was used in all initiator–monomer systems studied in this work.

Diffusion-Controlled Termination Reaction

Following the original model developments of Chiu et al.,[32] Achilias and Kiparissides[1] derived an analytical expression for the diffusion-controlled termination rate constant:

$$\frac{1}{k_t} = \frac{1}{k_{t0}} + \frac{r_t^2}{3} \frac{\lambda_0}{D_{pe}} \quad (30)$$

According to this model, the reciprocal of the effective rate constant, $1/k_t$, will be given by the sum of two terms. The first term, $1/k_{t0}$, represents the contribution of the intrinsic termination rate constant, k_{t0}, while the second term, $r_t^2\lambda_0/(3D_{pe})$, accounts for the diffusional phenomena related to the termination of growing polymer chains. Note that eq 30 is similar to eq 11 describing the variation of initiator efficiency with conversion.

To obtain a measure of the significance of the diffusional contribution relative to the intrinsic chemical term, we introduce two characteristic time constants, τ_{Dt} and τ_{Rt}, related to the corresponding diffusional and chemical term of eq 30.

$$\tau_{Dt} = r_t^2/3D_{pe} \qquad \tau_{Rt} = (k_{t0}\lambda_0)^{-1} \quad (31)$$

Accordingly, eq 30 is written in terms of τ_{Dt} and τ_{Rt} as

$$k_t = k_{t0}/(1 + \tau_{Dt}/\tau_{Rt}) \quad (32)$$

Thus, if diffusion of growing polymer chains controls the rate of termination, k_t will be smaller that the intrinsic rate constant k_{t0}.

$$\tau_{Dt} \gg \tau_{Rt}, \quad k_t < k_{t0} \quad (33)$$

On the other hand, if τ_{Dt} is much smaller than τ_{Rt}, then the termination rate constant, k_t, will remain constant.

$$\tau_{Dt} \ll \tau_{Rt}, \quad k_t \approx k_{t0} \quad (34)$$

The calculation of the parameters r_t and D_{pe}, which appear in the diffusion-controlled model (30), is discussed next.

Calculation of the Termination Radius r_t. r_t is an effective radius defining the reaction volume inside which termination of "live" polymer chains can occur. An estimation of r_t can be obtained by the following equation:[1,33]

$$r_t = [\ln [1000\tau^3/(N_A\lambda_0\pi^{3/2})]]^{1/2}/\tau \quad (35)$$

with

$$\tau = (3/2j_c\delta^2)^{1/2} \quad (36)$$

λ_0 denotes the total concentration of live radicals, and j_c is the entanglement spacing between polymer chains. j_c can be calculated by[1,33]

$$\frac{1}{j_c} = \frac{1}{j_{c0}} + \frac{2\varphi_p}{X_{c0}} \quad (37)$$

where φ_p is the polymer volume fraction. δ is the average root-mean-square end-to-end distance of a polymer chain, and X_{c0} is the critical degree of polymerization for the entanglement of polymer chains. The values of δ and X_{c0}

parameters have been tabulated[34,35] for a large number of polymers. The value of j_{c0} can be calculated from eqs 35–37 assuming that at time zero (i.e., $x = 0$ and $\varphi_p = 0$) the effective reaction radius, r_t, is equal to the hydrodynamic radius[36] of the polymer (R_H).

Calculation of the Effective Polymer Diffusion Coefficient D_{pe}. Termination of two live polymer chains follows actually a two-step process. Initially, live polymer chains move into close proximity by a pure translational diffusion process. Subsequently, the two active ends of the polymer chains reorient themselves (by segmental diffusion) to find each other and react. As a consequence, the effective diffusion coefficient of the polymer chains should include both translational and segmental contributions of the macromolecules.[37]

The translational diffusion coefficient can be assumed to be equal to the self-diffusion coefficient of the polymer, D_p, which is calculated from the generalized free-volume theory of Vrentas et al.[29]

$$D_p = (D_{p0}/M_w^2) \exp[-\gamma(\omega_m \hat{V}_m^* + \omega_p \hat{V}_p^* \xi_{13})/\xi_{13}\hat{V}_f] \quad (38)$$

Note that the dependence of the diffusion coefficient on the molecular weight follows the M_w^2 law according to the reptation theory.[1] M_w is the weight-average molecular weight of the polymer.

The value of D_{p0} is not usually known. In the present study, D_{p0} was calculated from eq 38 at zero polymer concentration.

$$D_p' = (D_{p0}/M_w'^2) \exp[-\gamma/(\xi_{13}V_{fm})] \quad (39)$$

Dividing eq 38 by eq 39, we obtain

$$D_p/D_p' = (M_w'^2/M_w^2) \exp[-(\gamma/\xi_{13})[(\omega_m \hat{V}_m^* + \omega_p \hat{V}_p^* \xi_{13})/\hat{V}_f] - (1/V_{fm})] \quad (40)$$

However, the polymer diffusion coefficient, D_p', at $\omega_p \to 0$ can be calculated from the Stokes–Einstein diffusion equation[38]

$$D_p' = k_B T/(6\pi\eta_s R_H) \quad (41)$$

where k_B is Boltzmann's constant, T is the absolute temperature, η_s is the viscosity of the monomer, and R_H is the hydrodynamic radius of the polymer.

To account for the segmental diffusion of the radical chains, the self-diffusion coefficient, D_p, is multiplied by the factor F_{seg}.[39] Therefore, the effective diffusion coefficient of the polymer, D_{pe}, will be given by

$$D_{pe} = F_{seg} D_p \quad (42)$$

The parameter F_{seg} accounts for the probability of two radicals to react when their active centers come into close proximity. North[39] has provided an analytical expression for the calculation of F_{seg} (see Table II).

Termination at High Monomer Conversions. At very high conversions, the self-diffusion coefficient of the polymer becomes very small, which results in an unrealistically low value of k_t according to eq 32. The reason for this unreasonably low value of k_t is that eq 38 does not account for the motion of the radical chains caused by the monomer propagation reaction.[40] Russell et al.[40] considered that, at very high conversions, the monomer propagation reaction contributes to the migration of a radical center, despite the actual translational immobility of the polymer chain as a whole. This phenomenon is known as "residual termination" or "reaction diffusion".[41]

Russell et al.[40] proposed two different models based on the chain end flexibility in order to calculate the residual termination rate constant $k_{t,res}$. Soh and Sundberg[33] used the volume swept out theory to develop a model for $k_{t,res}$. All models assume that the residual termination rate constant is proportional to the frequency of monomer addition to the radical chain end

$$k_{t,res} = A k_p[M] \quad (43)$$

Soh and Sundberg[34] provided the following equation for the proportionality parameter A:

$$A = f_t \pi r_t^2 \delta N_A/(1000 j_c^{1/2}) \quad (44)$$

where f_t is an efficiency factor. On the other hand, Russell et al.[40] derived two equations for the estimation of A. The first equation predicts a lower value for A, while the second one gives an upper value.

$$A = 4\pi\sigma\delta^2 N_A/(3 \times 1000) \quad (45)$$

$$A = 8\pi\delta^3 j_c^{1/2} N_A/(3 \times 1000) \quad (46)$$

Application of eqs 44–46 to an AIBN-initiated MMA polymerization at $T = 70$ °C and $[I]_0 = 0.01548$ mol/L yielded the following values for the proportionality constant A, respectively: 5.846, 0.703, and 9.353.

Note that the value of A calculated by the Soh and Sundberg equation lies between the lower and the upper value of A predicted by the Russell et al. equations. In the present work, the arithmetic average of A calculated by eqs 45 and 46 was used due to the fact that the chain end will be neither completely rigid nor totally flexible.

On the basis of the above theoretical considerations, the overall termination rate constant will be given by

$$k_{te} = k_t + k_{t,res} \quad (47)$$

Diffusion-Controlled Propagation Reaction

At very high conversions, even the movement of small molecules is restricted. As a result, the propagation reaction becomes diffusion-controlled. In the present work, the propagation rate constant follows exactly the same developments described in our previous paper.[1] Accordingly, k_p, is expressed in terms of the intrinsic propagation rate constant k_{p0} and a diffusion term accounting for diffusional limitations of the propagation reaction.

$$\frac{1}{k_p} = \frac{1}{k_{p0}} + \frac{r_m^2}{3}\frac{\lambda_0}{D_m} \quad (48)$$

The effective reaction radius r_m is assumed to be equal to the termination reaction r_t, while the monomer diffusion coefficient, D_m, is calculated from eq 24. In a similar way, we can define two characteristic time constants related to the diffusion of monomer molecules (τ_{Dp}) and its reaction (τ_{Rp}).

$$\tau_{Dp} = r_m^2/3D_m \qquad \tau_{Rp} = (k_{p0}\lambda_0)^{-1} \quad (49)$$

Using the characteristic times τ_{Dp} and τ_{Rp}, we write eq 48 as

$$k_p = k_{p0}/(1 + \tau_{Dp}/\tau_{Rp}) \quad (50)$$

Depending upon the significance of diffusion phenomena, one can obtain two limiting cases of eq 50:

$$\tau_{Dp} \gg \tau_{Rp}, \qquad k_p < k_{p0} \quad (51)$$

$$\tau_{Dp} \ll \tau_{Rp}, \qquad k_p \approx k_{p0} \quad (52)$$

In what follows, the general mathematical framework developed to describe diffusion-controlled initiation, propagation, and termination reactions is applied to the free-radical polymerization of MMA and styrene. Experimental results on total radical concentration, monomer conversion, and molecular weights reported by Zhu et al.[10] and O'Driscoll and Huang[42] are used to demonstrate the validity of the new theoretical developments.

Kinetic Model Developments

The free-radical polymerization of MMA can be described in terms of the following elementary reactions:

Initiation

$$I \xrightarrow{k_d} 2PR^{\bullet} + G\uparrow$$

$$PR^{\bullet} + M \xrightarrow{k_i} P^{\bullet}_1$$

Propagation

$$P^{\bullet}_n + M \xrightarrow{k_p} P^{\bullet}_{n+1}$$

Chain Transfer to Monomer

$$P^{\bullet}_n + M \xrightarrow{k_f} P^{\bullet}_1 + D_n$$

Termination by Combination

$$P^{\bullet}_n + P^{\bullet}_m \xrightarrow{k_{tc}} D_{n+m}$$

Termination by Disproportionation

$$P^{\bullet}_n + P^{\bullet}_m \xrightarrow{k_{td}} D_n + D_m$$

All symbols are described in the Nomenclature. For a well-stirred batch reactor, one can easily derive the following moment differential equations[37] to describe the progress of the reaction and molecular weight developments:

$$\frac{dI}{dt} = -k_d I - \frac{I}{V}\frac{dV}{dt} \tag{53}$$

$$\frac{d(PR^{\bullet})}{dt} = 2fk_d I - k_i(PR^{\bullet})M - \frac{(PR^{\bullet})}{V}\frac{dV}{dt} \tag{54}$$

$$\frac{dM}{dt} = -k_i(PR^{\bullet})M - (k_p + k_f)M\lambda_0 - \frac{M}{V}\frac{dV}{dt} \tag{55}$$

$$\frac{dV}{dt} = -V_0\epsilon[k_i(PR^{\bullet}) + (k_p + k_f)\lambda_0](1 - X) \tag{56}$$

$$\frac{d\lambda_0}{dt} = k_i(PR^{\bullet})M - k_t\lambda_0^2 - \frac{\lambda_0}{V}\frac{dV}{dt} \tag{57}$$

$$\frac{d\lambda_1}{dt} = k_i(PR^{\bullet})M - k_t\lambda_0\lambda_1 + k_pM\lambda_0 + k_fM(\lambda_0 - \lambda_1) - \frac{\lambda_1}{V}\frac{dV}{dt} \tag{58}$$

$$\frac{d\lambda_2}{dt} = k_i(PR^{\bullet})M - k_t\lambda_0\lambda_2 + k_pM(2\lambda_1 + \lambda_0) + k_fM(\lambda_0 - \lambda_2) - \frac{\lambda_2}{V}\frac{dV}{dt} \tag{59}$$

$$\frac{d\mu_0}{dt} = (k_{td} + {}^1/_2k_{tc})\lambda_0^2 + k_fM\lambda_0 - \frac{\mu_0}{V}\frac{dV}{dt} \tag{60}$$

$$\frac{d\mu_1}{dt} = k_t\lambda_0\lambda_1 + k_fM\lambda_1 - \frac{\mu_1}{V}\frac{dV}{dt} \tag{61}$$

$$\frac{d\mu_2}{dt} = k_t\lambda_0\lambda_2 + k_{tc}\lambda_1^2 + k_fM\lambda_2 - \frac{\mu_2}{V}\frac{dV}{dt} \tag{62}$$

where $\epsilon = (d_p - d_m)/d_p$ is the volume contraction factor.

In the present work we do not employ the two commonly used assumptions of quasi-steady-state approximation (QSSA) and long-chain hypothesis (LCH). Equations 53–62 were numerically integrated together with the appropriate diffusion models to obtain information on the variation of the total radical concentration, λ_0, monomer conversion

$$X = (M_0V_0 - MV)/(M_0V_0) \tag{63}$$

and the number-average and weight-average molecular weights of polymer.

$$\bar{M}_n = W_m(\mu_1/\mu_0) \qquad \bar{M}_w = W_m(\mu_2/\mu_1) \tag{64}$$

At the same time, the variation of f, k_t, and k_p with respect to polymerization time was calculated.

Application of the Diffusion Model to the MMA Polymerization

The numerical values of all parameters appearing in the kinetic model describing the free-radical polymerization of MMA are listed in Table I. Note that the values of k_{t0} and k_{p0} used in the present work are consistent with those recently obtained by Buback et al.,[43] Olaj and Schnöl-Bitai,[44] and Davis et al.[45] The physical and transport properties of the MMA–PMMA system are reported in Table II.

Results on the AIBN-Initiated Polymerization of MMA. In Figure 2, experimental results on conversion and total radical concentration for the AIBN-initiated free-radical polymerization of MMA are compared with model predictions. Discrete points represent experimental measurements reported by Zhu et al.[10] In the same figure, the gel effect index, GI = $(R_p/R_{p0} - 1)$, is also plotted with respect to polymerization time. As can be seen, there is an excellent agreement between experimental and predicted results for the total radical concentration although, at high conversions, model predictions of conversion are lower than the experimental measurements. This discrepancy might be due to nonisothermal polymerization conditions as discussed in the paper of O'Driscoll and Huang.[56] As Zhu et al.[22] noticed, the total polymerization time can be divided into four distinct regimes.

In the first stage of polymerization, the total radical concentration remains constant and the gel effect index, GI, is approximately zero. This stage is governed by the "classical" free-radical kinetics, and the kinetic rate constants, k_t and k_p (Figure 3), as well as the initiator efficiency, f, (Figure 4) remain constant. In the conversion range of 30–40%, the termination reaction becomes diffusion-controlled since it involves the simultaneous diffusion and reaction of two macroradicals. This results in a decrease of k_t according to eq 30, which is shown in Figure 3. A decrease in k_t brings about an increase in the gel effect index, GI, and in the total radical concentration as shown in Figure 2. During this stage of polymerization, k_p and f do not show any appreciable variation (see Figures 3 and 4). The observed large decrease in k_t is due to the substantial decrease of the translational diffusion coefficient of polymer chains (see eq 38). This phenomenon

Table I
Kinetic Rate Constants for the MMA Polymerization

$k_{p0} = 2.95 \times 10^7 \exp(-4353/RT)$ (L/(mol min)) (ref 46)
$k_{t0} = 5.88 \times 10^9 \exp(-701/RT)$ (L/(mol min)) (ref 46)
$k_f/k_p = 9.48 \times 10^3 \exp(-13880/RT)$ (ref 47)
$k_{tc}/k_{td} = 3.956 \times 10^{-4} \exp(4090/RT)$ (ref 48)

	Initiators			
parameter	AIBN	AIBME	AVN	LPO
f_0	0.58 (ref 49)	0.4 (ref 31)	0.6 (ref 51)	0.65 (ref 51)
k_d (min^{-1})	$6.32 \times 10^{16} \exp(-30660/RT)$ (ref 49)	$60 \exp(33.1 - 14800/T)$ (ref 31)	$60 \exp(34.4 - 14670/T)$ (ref 51)	$60 \exp(34.84 - 15400/T)$ (ref 51)
M_{jI}	68	100	110	155
V_I^* (cm^3/g)	0.913 (ref 30)	0.822 (ref 30)	0.96 (ref 30)	1.072 (ref 30)
ϵ_i/D_{I0} (s/cm^2)	372.38 (calcd)	$\epsilon_i = 1$, $D_{I0} = 0.0201$ cm^2/s (ref 50)	0.2323 (calcd)	1.06×10^{-4} (calcd)
γ_I	1.0	0.763 (ref 1)	1.0	1.0

Table II
Physical and Transport Properties for the MMA–PMMA System

$d_m = 0.968 - 1.225 \times 10^{-3}T$ (°C) (g/cm^3) (ref 1)
$d_p = d_m(1 + \epsilon)$; $\epsilon = 0.183 + 9.0 \times 10^{-4}T$ (°C) (ref 1)
$V_{fm} = 0.149 + 2.9 \times 10^{-4}T$ (°C) (ref 34)
$V_{fp} = 0.0194 + 1.3 \times 10^{-4}(T - 105)$; $T < 105$ °C (ref 34)
$V_m^* = 0.822$ (cm^3/g) (ref 30); $V_p^* = 0.77$ (cm^3/g) (ref 52)
$M_{jm} = W_m = 100.13$; $M_{jp} = 150$
$\gamma = 0.763$ (ref 1); $\delta = 6.9$ (Å) (ref 35); $X_{c0} = 100$ (ref 34)
$F_{seg} = r_e^3[\pi r_e + 6(2^{1/2})a_{seg}r_B]/(16\pi r_B^4)$ (ref 39)
$r_e = 17$ (Å) (Kuhn's segment length) (ref 53)
$a_{seg} = 0.28$ (for AIBN); $a_{seg} = 1.024$ (for AIBME) (calcd)
$r_B = (R_H)_0$
$D_{m0} = 0.827 \times 10^{-10}$ (cm^2/s) (ref 1)
$\eta_s = \exp(-0.099 + 496/T\,(K) - 1.5939 \ln [T\,(K)])$ (Pa s) (ref 54)
$R_H = 1.3 \times 10^{-9} M_w^{0.574}$ (cm) (ref 55)

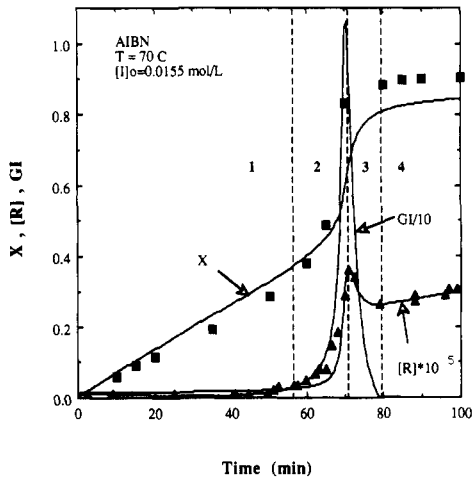

Figure 2. Conversion (X), total radical concentration ([R]), and gel effect index (GI) versus time for the AIBN-initiated bulk polymerization of MMA (experimental data points: (▲, ■) ref 10).

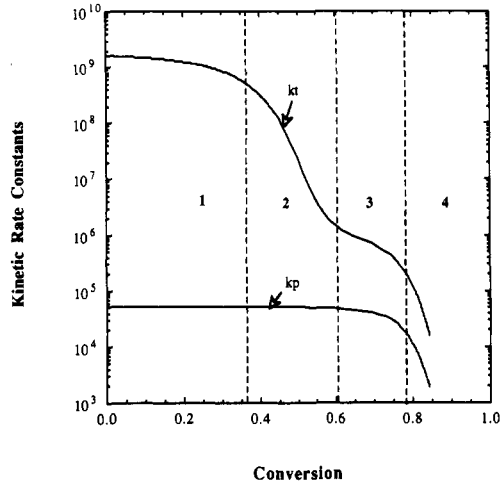

Figure 3. Termination (k_t) and propagation (k_p) rate constants for the AIBN-initiated bulk polymerization of MMA (conditions same as in Figure 2).

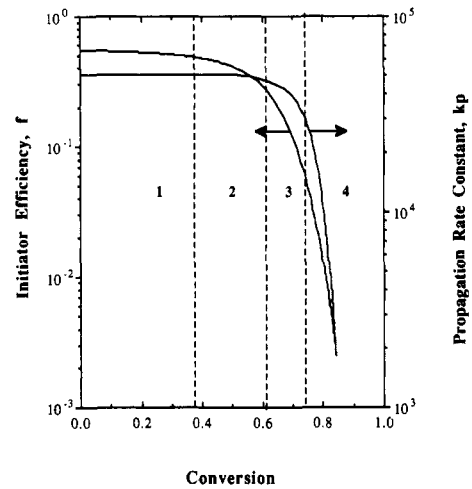

Figure 4. Initiator efficiency (f) and propagation rate constant (k_p) for the AIBN-initiated bulk polymerization of MMA (conditions same as in Figure 2).

is known as the gel effect. The maxima in the total radical concentration and the gel effect index mark the crossover from stage 2 to stage 3 of the polymerization. In this region, the total radical population decreases as well as the polymerization rate. This unusual change in [R•] can be explained by the results of Figures 3 and 4. It can be seen that, although the effect on k_p is relatively small, there is a rather sharp decrease in the initiator efficiency, f, due to the large decrease of primary radical diffusion coefficient according to eq 21. Therefore, the diffusion of primary radicals out of their cages is substantially hindered. As a result, the number of initiator primary radicals which are able to initiate new polymer chains falls. During this stage, the observed decrease in k_t is not as abrupt as in stage 2. Actually, in stage 3 the translational diffusion coefficient of "live" chains becomes very small, and any movement of growing polymer chains is attributed to the "residual termination" diffusion. During this stage, the decrease in k_t will be proportional to the decrease in k_p according to eq 43. In summary, we can say that the passage from stage 2 to stage 3 is marked by the appearance of two important physical phenomena associated with the initiator efficiency and the termination rate constant. In stage 3, the significant change in f is attributed to the decrease of primary radical diffusion coefficient, while the observed variation in k_t has been linked to the residual termination phenomenon.

Finally, at conversions about 80% the total radical population starts slowly to increase up to the final conversion. During this stage of polymerization, both k_p and f significantly fall while the polymerization rate becomes approximately zero. The observed increase in

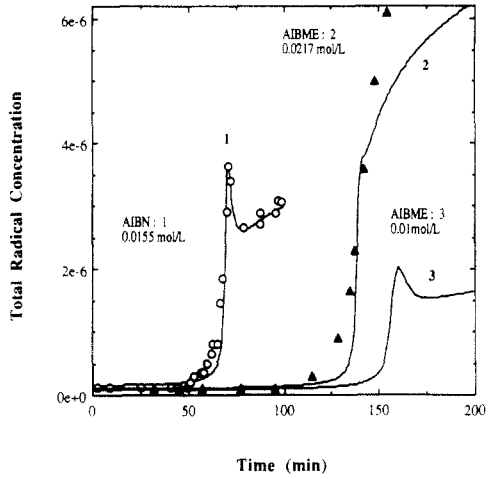

Figure 5. Total radical concentration for the bulk polymerization of MMA for different initiator types and concentrations (experimental data points: (○) ref 10; (▲) ref 25).

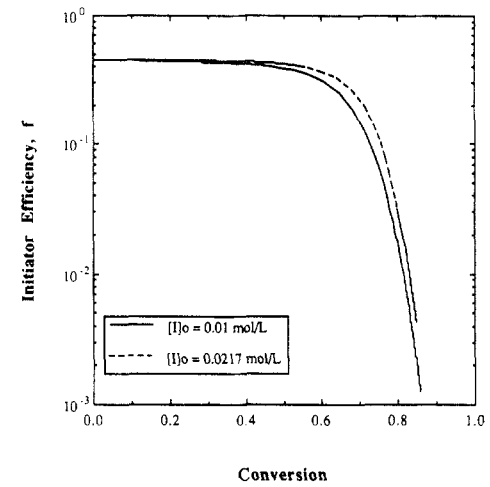

Figure 6. Initiator efficiency (f) versus conversion for the AIBME-initiated MMA polymerization at different initial initiator concentrations.

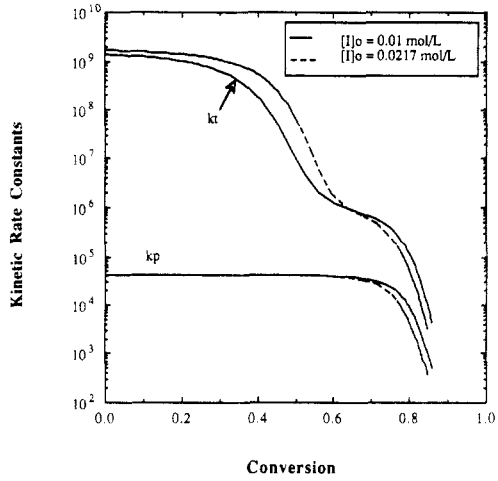

Figure 7. Termination (k_t) and propagation (k_p) rate constants versus conversion for the AIBME-initiated MMA polymerization at different initial initiator concentrations.

the total radical population is due to a further reduction of k_t as shown in Figure 3. This rather unusual behavior of k_t with conversion can also be seen in the experimental data of Zhu et al.,[26] Buback,[57] and Shen et al.[58]

Results on the AIBME-Initiated Polymerization of MMA. In general, for the calculation of the variation of initiator efficiency with conversion, one needs to know the diffusion coefficient of the primary radicals, D_{I0}, at $t = 0$ as well as the initiation rate constant, k_{i0} ($=\epsilon_i k_{p0}$), or, otherwise, the parameter ϵ_i. Note that the ratio ϵ_i/D_{I0} can be calculated from the application of the initial condition (28), which means that at zero conversion the initiator efficiency will be $f = f_0$.

For the AIBME-initiated polymerization of MMA, we assumed that $k_{i0} \cong k_{p0}$ and $D_{I0} \cong D_{m0}$ due to the similarity of AIBME primary radicals to the chain end of the growing polymer chains.

The free-radical polymerization of MMA was simulated using our general diffusion model for the experimental conditions of O'Driscoll and Huang[42,56] (T = 60 °C, $[I]_0$ = 0.01 mol/L) and those reported by Shen et al.[25] (T = 60 °C, $[I]_0$ = 0.0217 mol/L). In Figure 5, the total radical concentration is plotted with respect to time for two different AIBME concentrations. Both results are compared to the variation of the total radical concentration obtained for the AIBN-initiated polymerization of MMA. Curve 2 represents the experimental conditions of Shen et al.,[25] while curve 3 refers to the experimental conditions of O'Driscoll and Huang.[42,56] Discrete points in curves 1 and 2 represent experimental data. It is important to point out that the total radical concentration for the experimental conditions of curve 3 shows a similar behavior to the variation of [R•] observed for the AIBN-initiated polymerization of MMA. On the other hand, the AIBME-initiated polymerization of MMA, at higher initiator concentrations, exhibits a monotonous increase with time (curve 2). To explain the observed difference in the variation of the total radical concentration with initiator concentration, the initiator efficiency, f, and the termination and propagation rate constants, k_t and k_p, are plotted with respect to monomer conversion (Figures 6 and 7) for the two initial initiator concentrations ($[I]_0$ = 0.01 mol/L and $[I]_0$ = 0.0217 mol/L). As can be seen from the results of Figure 6, at high initiator concentrations, the decrease in f with conversion is smaller than that estimated at the lower initiator concentration, $[I]_0$ = 0.01 mol/L. This difference in the variation of f with conversion can be explained by the fact that the average chain length decreases with initiator concentration. A smaller average chain length will result in a decrease of the characteristic time τ_{DI} (see eq 12) due to the simultaneous decrease of r_2 and increase in D_I. Therefore, at higher initiator concentrations, diffusion of primary radicals will be less hindered than at lower initiator concentrations. The chain length dependence of the characteristic time constants, τ_{Dt} and τ_{Dp}, can also be invoked to explain the calculated variation of k_p and k_t with respect to the initiator concentration (Figure 7). It is apparent from the results of Figures 6 and 7 that the initial initiator concentration will affect the rate constants of all diffusion-controlled reactions. This is a rather important result obtained by the application of the new model to the bulk polymerization of MMA.

Subsequently, we examine the dependence of initiator efficiency on the chemical structure of the initiator molecules.

Dependence of f on Initiator Type. To show the dependence of initiator efficiency, f, upon the chemical structure of the initiator, the free-radical polymerization of MMA was examined for three different initiators, namely, 2,2′-azobis(isobutyronitrile) (AIBN), 2,2′,4,4′-tetramethyl-2,2′-azovaleronitrile (AVN), and dilauroyl peroxide (LPO).

Figure 8 illustrates the variation of f with conversion for the three initiators. In all simulation runs, the polymerization temperature was T = 70 °C and the initial

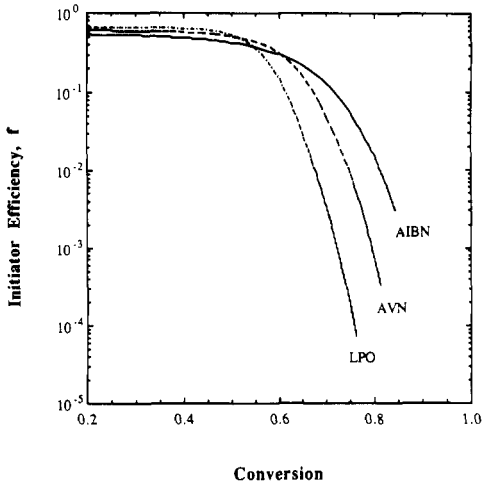

Figure 8. Dependence of initiator efficiency upon the type of initiator (conditions same as in Figure 2).

initiator concentration was $[I]_0 = 0.01548$ mol/L. The values of the ϵ_i/D_I parameter calculated from the application of the initial condition (28) are reported in Table I. The results of Figure 8 show that the initiator efficiency does depend on the initiator type, especially at high monomer conversions. It is important to mention that a similar behavior for the initiator efficiency was reported by Russell et al.[20] The observed variation of f with conversion and initiator type can be explained by examining the value of the molar volume $\hat{V}_I^* M_{jI}$ parameter for the three investigated initiators. The term $\hat{V}_I^* M_{jI}$ appears in eq 21 and describes the dependence of diffusion coefficient of primary radicals upon the size of initiator fragments and the free volume of the reacting medium. For the initiators studied in this work, their molar volumes are as follows:

initiator type	$\hat{V}_I^* M_{jI}$, cm³/mol
AIBN	0.913 × 68 = 62.1
AVN	0.96 × 110 = 105.6
LPO	1.072 × 155 = 166.2

As can be seen the molar volume $\hat{V}_I^* M_{jI}$ increases with the size of the initiator molecule. Thus, the LPO molecules will have a larger molar volume than the AIBN and AVN initiators. Therefore, according to eq 21, the diffusion coefficient of LPO primary radicals will be significantly lower than the diffusion coefficient of AIBN and AVN radicals. A lower diffusion coefficient results in a large increase of the characteristic time constant τ_{DI} (eq 12), which brings about a decrease in f according to eq 13.

Prediction of Conversion and Average Molecular Weights. The ability of the present model to predict monomer conversion and molecular weight developments is demonstrated in Figures 9–11. In Figure 9, experimental data on conversion obtained by O'Driscoll and Huang[56] are compared to model predictions of conversion shown by the continuous line. Two sets of experimental points are plotted in Figure 9, which correspond to the type of ampules employed by O'Driscoll and Huang to maintain isothermal polymerization conditions. Notice that experimental conversion values obtained with ordinary ampules (i.e., squares in Figure 9) are higher than conversion values measured in annular ampules (i.e., circles in Figure 9). The reason is that, in ordinary ampules, it is more difficult to maintain a constant polymerization temperature due to the limited heat-transfer area of the regular cylindrical ampules. As a result, the measured polymerization rate in regular ampules might be higher

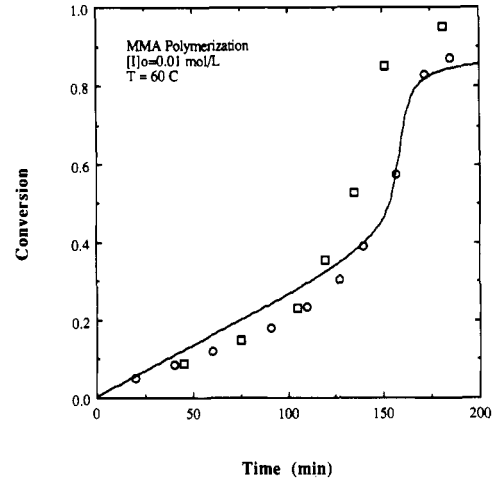

Figure 9. Conversion versus time for the bulk polymerization of MMA using AIBME as initiator (experimental data points:[56] (○) annular ampules; (□) ordinary ampules).

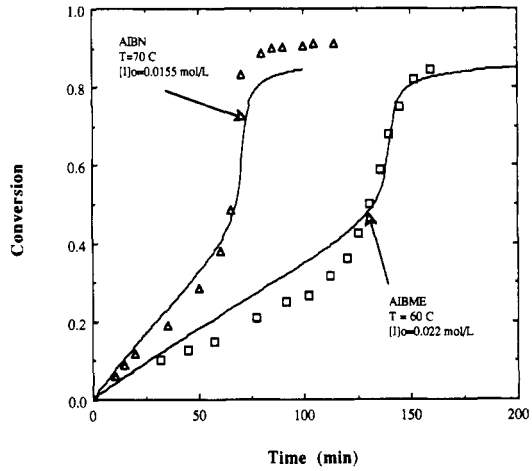

Figure 10. Conversion versus time for the bulk polymerization of MMA using AIBME and AIBN as initiators (experimental data points: (△) ref 10; (□) ref 42).

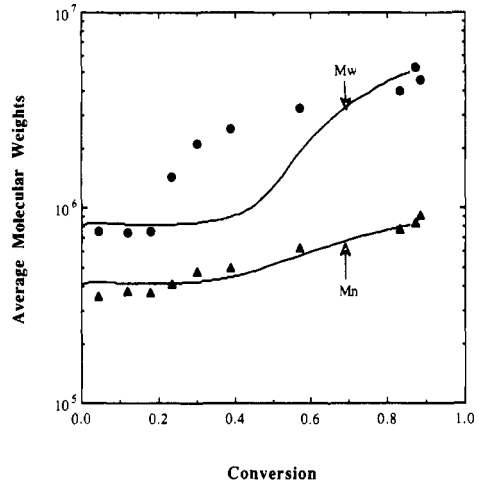

Figure 11. Weight-average ($\bar{M}_w$) and number-average ($\bar{M}_n$) molecular weight for the AIBME-initiated bulk polymerization of MMA at $T = 60$ °C and $[I]_0 = 0.01$ mol/L (experimental data points: ref 42).

than the one measured in annular ampules in which isothermal conditions can be more easily established. Note that the predicted conversion values agree with experimental conversion data obtained in annular (i.e., isothermal) ampules.

In Figure 10, experimental conversion measurements reported by Zhu et al.[10] and O'Driscoll and Huang[42] are

Table III
Kinetic Rate Constants for the Styrene Polymerization

$k_{p0} = 6.54 \times 10^8 \exp(-7051/RT)$ (L/(mol min)) (ref 46)
$k_{t0} = 1.022 \times 10^{11} \exp(-2268/RT)$ (L/(mol min)) (ref 46)
$k_{fm}/k_p = 1.0 \exp(-3212/T)$ (ref 59)
$k_{tc} = k_t$; $k_{td} = 0$

Initiator

parameter	AIBME
f_0	0.4 (ref 42)
k_d (s^{-1})	$\exp(36.8 - 16100/T)$ (ref 42)
M_{jI}	100
$\hat{V}_I^*$ (cm^3/g)	0.822 (ref 30)
ϵ_i/D_{I0} (s/cm^2)	31.04 (calcd)
γ_I	1.0

Table IV
Physical and Transport Properties for the St–PSt System

$d_m = 0.9236 - 0.887 \times 10^{-3}T$ (°C) (g/cm^3) (ref 34)
$d_p = d_m(1 + \epsilon)$; $\epsilon = 0.137 + 4.4 \times 10^{-4}T$ (°C) (ref 34)
$V_{fm} = 0.112 + 6.2 \times 10^{-4}T$ (°C) (ref 34)
$V_{fp} = 0.0245 + 1.4 \times 10^{-4}(T - 82)$, $T < 82$ °C (ref 34)
$\hat{V}_m^* = 0.846$ (cm^3/g) (ref 30); $\hat{V}_p^* = 0.85$ (cm^3/g) (ref 52)
$M_{jm} = W_m = 104.14$; $M_{jp} = 163$ (ref 52)
$\gamma = 0.999$ (ref 1); $\delta = 7.4$ (Å) (ref 35); $X_{c0} = 385$ (ref 34)
$F_{seg} = r_e^3[\pi r_e + 6(2^{1/2})a_{seg}r_B]/(16\pi r_B^4)$ (ref 39)
$r_e = 16.9$ (Å) (Kuhn's segment length (ref 53)
$a_{seg} = 0.097$ (calcd)
$r_B = (R_H)_0/r$
$D_{m0} = 1.97 \times 10^{-8}$ (cm^2/s)
$\eta_s = \exp(-22.673 + 1758/T\,(K) + 1.67 \ln (T\,(K)))$ (Pa s) (ref 54)
$R_H = 1.31 \times 10^{-9}M_w^{0.56}$ (cm) (ref 38)

compared to model predictions (i.e., continuous lines). It is clear that the present model has the ability to closely simulate experimental conversion data obtained by different laboratories without the need to resort to any kind of parameter fitting.

In Figure 11, predicted number-average and weight-average molecular weights are compared to experimental data reported by O'Driscoll and Huang.[42] It can be seen that the prediction of $\bar{M}_n$ is very good. On the other hand, the model fails to predict $\bar{M}_w$ values in the conversion range of 20–60%. According to a recent publication by Zhu and Hamielec,[21] one could satisfactorily predict the experimental variation in $\bar{M}_w$ by considering two termination rate constants (i.e., k_{tn} and k_{tw}), one depending on the number-average and the other on the weight-average chain length of the terminating polymer molecules.

Application of the Diffusion Model to the Styrene Polymerization. To demonstrate the general application of the new diffusion model to other polymerization systems, we investigated the bulk free-radical polymerization of styrene. The numerical values of the kinetic rate constants for the styrene polymerization are given in Table III. Table IV contains the physical and transport properties of the St–PSt system.

In Figure 12, experimental conversion values are compared to model predictions. The discrete points represent conversion data obtained by O'Driscoll and Huang[42] for the AIBME-initiated isothermal (T = 60 °C) polymerization of styrene. Clearly, there is a good agreement between experimental and predicted results. The variation in the total radical concentration with time is also plotted in Figure 12. It is interesting to see that the total initiator concentration exhibits a similar behavior to the one observed for the AIBN-initiated polymerization of MMA.

Finally, in Figure 13, predicted values of polydispersity index are compared to experimental measurements.[42] It is apparent that the proposed model can satisfactorily predict molecular weight developments related to the free-radical bulk polymerization of styrene.

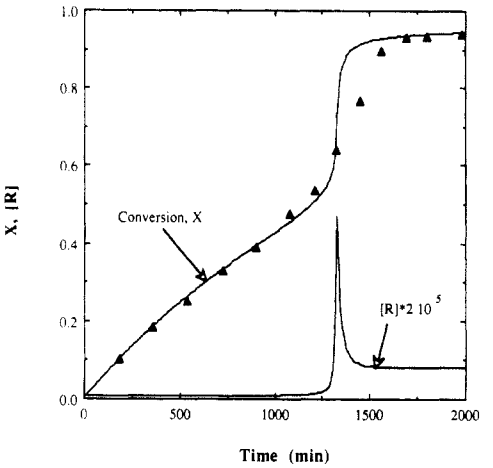

Figure 12. Conversion (X) and total radical concentration ([R•]) versus time for the AIBME-initiated bulk polymerization of styrene at T = 60 °C and $[I]_0$ = 0.01 mol/L (experimental data points: ref 42).

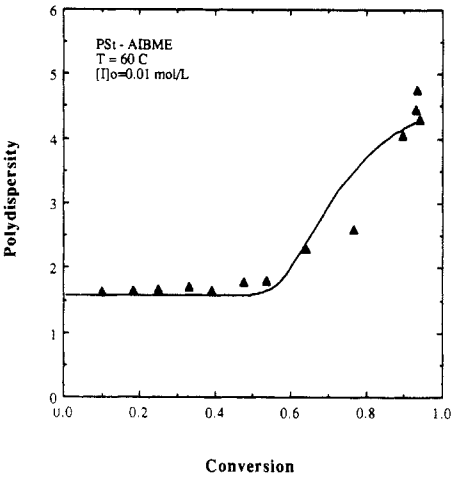

Figure 13. Polydispersity versus conversion for the AIBME-initiated bulk polymerization of styrene (conditions same as in Figure 12). Experimental data points: ref 42.

Conclusions

A new theoretical modeling approach has been developed to describe diffusion-controlled reactions in free-radical polymerization. A new model has been developed for calculating the initiator efficiency during polymerization. Equations for the prediction of the variation of termination and propagation rate constants have been derived based on our previous work[1] and the generalized free-volume theory of Vrentas and Duda.[27-29] All parameters appearing in the new diffusion model have a clear physical meaning and can be estimated in terms of physical and transport properties of the monomer–polymer–initiator system. Characteristic time constants related to the initiation, termination, and propagation reactions have been defined in an attempt to quantify the importance of diffusion-controlled phenomena in free-radical kinetics. Furthermore, the new model does not need the introduction of critical break points to mark the onset of various diffusion-controlled phenomena. A physical explanation of the gel, glass, and cage effects has also been offered.

Simulation results show that the present model is capable of accurately predicting the total "live" radical concentration change during the polymerization as well as the monomer conversion and the number- and weight-average molecular weights. The present model has been applied to the bulk polymerization of MMA and styrene initiated by various initiators including AIBN, AIBME,

AVN, and LPO. To our knowledge, this is the first attempt which considers simultaneously the variation of f, k_p, and k_t due to the appearance of diffusion-controlled phenomena. Current research efforts are focused on the extension of the model to diffusion-controlled copolymerization reactions.

Acknowledgment. This work was partially supported by the CPERI and the EEC under the BRITE Project P-1560.

Nomenclature

A	proportionality constant
AIBME	2,2′-azodiisobutyrate
AIBN	2,2′-azobis(isobutyronitrile)
AVN	2,2′,4,4′-tetramethyl-2,2′-azovaleronitrile
D	diffusion coefficient
d	density
D_n	concentration of a "dead" polymer with n monomer units
f	efficiency of the initiator
G	gas molecule
I	concentration of the initiator
j_c	entanglement spacing
k_B	Boltzmann's constant (1.3806×10^{-23} J/K)
k_d	initiator decomposition rate constant
k_f	chain transfer to monomer rate constant
k_i	rate constant for the initiation reaction
k_p	rate constant for the propagation reaction
k_t	total rate constant for the termination reaction ($k_{tc} + k_{td}$)
k_{tc}	termination by combination rate constant
k_{td}	termination by disproportionation rate constant
l_0	segment length
LPO	dilauroyl peroxide
M	monomer concentration
M_j	molecular weight of the jumping unit
MMA	methyl methacrylate
$\bar{M}_n$, $\bar{M}_w$	number- and weight-average molecular weight
n	number of monomer units in a polymer segment
N_A	Avogadro's number (6.023×10^{23})
P_n	concentration of a "live" radical with n monomer units
PR$^\bullet$	primary radical
R	universal gas constant
r	effective reaction radius
R_H	hydrodynamic radius
r_m	monomer radius
St	styrene
T	temperature
t	time
V	volume of the reactor
V_f	free volume of the mixture
W_m	molecular weight of the monomer
X	conversion
X_{C0}	critical degree of polymerization for entanglements of the pure polymer

Greek Letters

γ	overlap factor
δ	average root-mean-square end-to-end distance per square root of the number of monomer units in a chain
ϵ	volume contraction factor at 100% conversion
ϵ_i	$=k_{i0}/k_{p0}$
η_s	solvent viscosity
λ_i	moments of the growing radical distribution (i = 0, 1, 2)
μ_i	moments of the "dead" polymer distribution (i = 0, 1, 2)
ξ	ratio of the critical molar volume of the jumping unit to the critical molar volume of the polymer
σ	Lennard-Jones radius
τ	characteristic time
φ	volume fraction
ω	weight fraction

Subscripts

D	diffusion limited
eff	effective
I	initiator
i	initiation
m	monomer
o	initial conditions
p	polymer
r	reaction limited
res	residual termination
t	termination

Superscripts

^	specific
*	critical
′	concentration in the bulk phase
•	radical

References and Notes

(1) Achilias, D.; Kiparissides, C. *J. Appl. Polym. Sci.* **1988**, *35*, 1303.
(2) Mita, I.; Horie, K. *J. Macromol. Sci., Rev. Macromol. Chem. Phys.* **1987**, *C27* (1), 91.
(3) North, A. M. *The Collision Theory of Chemical Reactions in Liquids*; Wiley: New York, 1964.
(4) North, A. M. *The Kinetics of Free Radical Polymerization.* In *The International Encyclopedia of Physical Chemistry and Chemical Physics*; Bawn, C. E. H., Ed.; Pergamon Press: London, 1966; Vol. 1.
(5) North, A. M. *Diffusion Control of Homogeneous Free Radical Reactions.* In *Progress in High Polymers*; Robb, J. C., Peaker, F. W., Eds.; CRC Press: Cleveland, OH, 1968; Vol. 2.
(6) Noyes, R. M. *Cage Effect.* In *Encyclopedia of Polymer Science and Technology*; Mark, H. F., Gaylord, N. G., Bikales, N. M., Eds.; Wiley-Interscience: New York, 1965; Vol. 2, p 796.
(7) Brooks, B. W. *Proc. R. Soc. London, A* **1977**, *357*, 183.
(8) De Schrijver, F.; Smets, G. *J. Polym. Sci., Part A-1* **1966**, *4*, 2201.
(9) Shen, J.; Tian, Y.; Wang, G.; Yang, M. *Sci. China* **1990**, *B33*, 1046.
(10) Zhu, S.; Tian, Y.; Hamielec, A. E.; Eaton, D. R. *Polymer* **1990**, *31*, 154.
(11) Sack, R.; Schulz, G.-V.; Meyerhoff, G. *Macromolecules* **1988**, *21* (12), 3345.
(12) Garcia-Rubio, L. H.; Mehta, J. *ACS Symp. Ser.* **1986**, *313*, 202.
(13) O'Driscoll, K. F.; Ghosh, P. *Initiation in Free Radical Polymerization.* In *Structure and Mechanism in Vinyl Polymerization*; Tsuruta, T., O'Driscoll, K. F., Eds.; Marcel Dekker: New York, 1969.
(14) Biesenberger, J. A.; Sebastian, D. H. *Principles of Polymerization Engineering*; J. Wiley and Sons: New York, 1983.
(15) Arai, K.; Saito, S. *J. Chem. Eng. Jpn.* **1976**, *9*, 302.
(16) Arai, K.; Yamaguchi, H.; Saito, S.; Sarashina, E.; Yamamoto, T. *J. Chem. Eng. Jpn.* **1986**, *19*, 413.

(17) Stickler, M. *Makromol. Chem.* **1983**, *184*, 2563.
(18) Denisov, E. T. *Makromol. Chem., Suppl.* **1984**, *8*, 63.
(19) Ito, K. *Polym. J.* **1985**, *17*, 421.
(20) Russell, G. T.; Napper, D. H.; Gilbert, R. G. *Macromolecules* **1988**, *21*, 2141.
(21) Zhu, S.; Hamielec, A. E. *Macromolecules* **1989**, *22*, 3093.
(22) Balke, S. T.; Hamielec, A. E. *J. Appl. Polym. Sci.* **1973**, *17*, 905.
(23) Ballard, M. J.; Gilbert, R. G.; Napper, D. H.; Pomery, P. J.; O'Sullivan, P. W.; O'Donnell, J. H. *Macromolecules* **1986**, *19*, 1303.
(24) Kamachi, M. *Adv. Polym. Sci.* **1987**, *82*, 207.
(25) Shen, J.; Tian, Y.; Zeng, Y.; Qiu, Z. *Makromol. Chem., Rapid Commun.* **1987**, *8*, 615.
(26) Zhu, S.; Tian, Y.; Hamielec, A. E.; Eaton, D. R. *Macromolecules* **1990**, *23*, 1144.
(27) Vrentas, J. S.; Duda, J. L. *J. Polym. Sci., Polym. Phys. Ed.* **1977**, *15*, 403.
(28) Vrentas, J. S.; Duda, J. L. *J. Polym. Sci., Polym. Phys. Ed.* **1977**, *15*, 417.
(29) Vrentas, J. S.; Duda, J. L.; Ling, H.-C. *J. Polym. Sci., Polym. Phys. Ed.* **1984**, *22*, 459.
(30) Haward, R. N. *J. Macromol. Sci., Rev. Macromol. Chem.* **1970**, *C4*, 191.
(31) Stickler, M. *Makromol. Chem.* **1986**, *187*, 1765.
(32) Chiu, W. Y.; Carratt, G. M.; Soong, D. S. *Macromolecules* **1983**, *16*, 348.
(33) Soh, S. K.; Sundberg, D. C. *J. Polym. Sci., Polym. Chem. Ed.* **1982**, *20*, 1315.
(34) Soh, S. K.; Sundberg, D. C. *J. Polym. Sci., Polym. Chem. Ed.* **1982**, *20*, 1345.
(35) Ferry, J. D. *Viscoelastic Properties of Polymers*, 3rd ed.; Wiley: New York, 1980.
(36) De Gennes, P.-G. *J. Chem. Phys.* **1982**, *76* (6), 3322.
(37) Louie, B. M.; Carratt, G. M.; Soong, D. S. *J. Appl. Polym. Sci.* **1985**, *30*, 3985.
(38) Varma, B. K.; Fujita, Y.; Takahashi, M.; Nose, T. *J. Polym. Sci., Polym. Phys. Ed.* **1984**, *22*, 1781.
(39) North, A. M. *Makromol. Chem.* **1965**, *83*, 15.
(40) Russell, G. T.; Napper, D. H.; Gilbert, R. G. *Macromolecules* **1988**, *21*, 2133.
(41) Schulz, G. V. *Z. Phys. Chem. (Frankfurt am Main)* **1956**, *8*, 290.
(42) O'Driscoll, K. F.; Huang, J. *Eur. Polym. J.* **1989**, *25* (7/8), 629.
(43) Buback, M.; Garcia-Rubio, L. H.; Gilbert, R. G.; Napper, D. H.; Guillot, J.; Hamielec, A. E.; Hill, D.; O'Driscoll, K. F.; Olaj, O. F.; Shen, J.; Solomon, D.; Moad, G.; Stickler, M.; Tirrell, M.; Winnik, M. A. *J. Polym. Sci., Polym. Lett.* **1988**, *26*, 293.
(44) Olaj, O. F.; Schnöll-Bitai, I. *Eur. Polym. J.* **1989**, *25* (7/8), 635.
(45) Davis, T. P.; O'Driscoll, K. F.; Piton, M. C.; Winnik, M. A. *Macromolecules* **1989**, *22*, 2785.
(46) Mahabadi, H. K.; O'Driscoll, K. F. *J. Macromol. Sci., Chem.* **1977**, *A11* (5), 967.
(47) Stickler, M.; Meyerhoff, G. *Makromol. Chem.* **1978**, *179*, 2729.
(48) Bevington, J. C.; Melville, H. W.; Taylor, R. P. *J. Polym. Sci.* **1954**, *14*, 463.
(49) Tobolsky, A. V.; Baysal, B. *J. Polym. Sci.* **1953**, *11*, 471.
(50) Duda, J. L.; Vrentas, J. S.; Ju, S. T.; Liu, H. T. *AIChE J.* **1982**, *28* (2), 279.
(51) Panke, D.; Stickler, M.; Wunderlich, W. *Makromol. Chem.* **1983**, *184*, 175.
(52) Liu, H. T.; Duda, J. L.; Vrentas, J. S. *Macromolecules* **1980**, *13*, 1587.
(53) Aharoni, S. M. *Macromolecules* **1986**, *19*, 426.
(54) Design Institute for Physical Property Data AIChE. *Data Compilation Tables of Properties of Pure Compounds*; Daubert, T. E., Danner, R. P., Eds.; The Pennsylvania State University: University Park, PA, 1985.
(55) Balloge, S. J. Ph.D. Thesis, University of Minnesota, Minneapolis, MN, 1986.
(56) O'Driscoll, K. F.; Huang, J. *Eur. Polym. J.* **1990**, *26* (6), 643.
(57) Buback, M. *Makromol. Chem.* **1990**, *191*, 1575.
(58) Shen, J.; Tian, Y.; Wang, G.; Yang, M. *Sci. China* **1990**, *B33*, 1040.
(59) Brandrup, J.; Immergut, E., Eds. *Polymer Handbook*; Wiley-Interscience: New York, 1971.

Registry No. AIBN, 78-67-1; AIBME, 2589-57-3; AVN, 4419-11-8; LPO, 2895-03-6; St, 100-42-5; MMA, 80-62-6.